

Chapter 14

REX CHERT MEMBER OF THE PERMIAN PHOSPHORIA FORMATION: COMPOSITION, WITH EMPHASIS ON ELEMENTS OF ENVIRONMENTAL CONCERN

J.R. HEIN, B.R. McINTYRE, R.B. PERKINS, D.Z. PIPER and J.G. EVANS

ABSTRACT

We present bulk chemical and mineralogical compositions, as well as petrographic and outcrop descriptions, of rocks collected from three measured outcrop sections of the Rex Chert Member of the Phosphoria Formation in southeast Idaho. The three measured sections were chosen from 10 outcrops of Rex Chert that were described in the field. The Rex Chert overlies the Meade Peak Phosphatic Shale Member of the Phosphoria Formation, the source of phosphate ore in the region. Rex Chert removed as overburden constitutes part of the material transferred to waste-rock piles during phosphate mining. It is also used to surface roads in the mining district. It has been proposed that the chert be used to cap and isolate waste piles, thereby inhibiting the leaching of potentially toxic elements into the environment. The rock samples studied here are from individual chert beds representative of each stratigraphic section sampled. The Cherty Shale Member of the Phosphoria Formation that overlies the Rex Chert in measured section 1 and the upper Meade Peak and the transition zone to the Rex Chert in section 7 were also described and sampled.

The cherts are predominantly spiculite composed of granular and mosaic quartz, and sponge spicules, with various but minor amounts of other fossils and detrital grains. The Cherty Shale Member and transition rocks between the Meade Peak and Rex Chert are siliceous siltstones and argillaceous cherts with ghosts of sponge spicules and somewhat more detrital grains than the chert. The dominant mineral is quartz. Carbonate beds are rare in each section and are composed predominantly of calcite and dolomite in addition to quartz. Feldspar, mica, clay minerals, calcite, dolomite, and carbonate fluorapatite are minor to trace minerals in the chert.

The concentration of SiO₂ in the chert averages 94.6 wt.%. Organic-carbon content is generally very low, but can be as much as 1.8% in Cherty Shale Member samples and as much as 3.3% in samples from the transition between the Meade Peak and Rex Chert. Likewise, phosphate (P₂O₅) is generally low in the chert, but can be as much as 3.1% in individual chert beds. Selenium concentrations in Rex Chert and Cherty Shale Member samples vary from <0.2 to 138 ppm, with a mean concentration of 7.0 ppm. This mean Se content is heavily dependent on two values of 101 and 138 ppm for siliceous siltstone from

the lower part of the Rex Chert, which contains rocks that are transitional in character between the Meade Peak and Rex Chert Members. Without those two samples, the mean Se concentration is <1.0 ppm. Other elements of environmental interest, As, Cr, V, Zn, Hg, and Cd, generally occur in concentrations near or below that in average continental shale. Stratigraphic changes, equivalent to temporal changes in the depositional basin, in chemical composition of rocks are notable either as uniform changes through the sections or as distinct differences in the mean composition of rocks that comprise the upper and lower halves of the sections.

Q-mode factors are interpreted to represent the following rock and mineral components: chert-silica component consisting of Si (\pm Ba); phosphorite-carbonate fluorapatite component composed of P, Ca, As, Y, V, Cr, Sr, and La (\pm Fe, Zn, Cu, Ni, Li, Se, Nd, Hg); shale component composed of Al, Na, Zr, K, Ba, Li, and organic C (\pm Ti, Mg, Se, Ni, Fe, Sr, V, Mn, Zn); carbonate component (dolomite, calcite, silicified carbonates) composed of carbonate C, Mg, Ca, and Si (\pm Mn); and, tentatively, organic matter-hosted elements (and/or sulfide-sulfate phases) composed of Cu (\pm organic C, Zn, Mn, Si, Ni, Hg, Li). Selenium shows a dominant association with organic matter and to lesser degrees associations with other shale components and carbonate fluorapatite. Consideration of larger numbers of factors in Q-mode analysis indicates that native Se (a factor containing Se (\pm Ba)) may also comprise a minor component of the Se complement.

Comparison of our data with those from newly exposed outcrops in active phosphate mines indicates that weathering of typical Rex Chert outcrops likely plays an important role in removing environmentally sensitive elements.

INTRODUCTION

The Rex Chert Member conformably overlies the Meade Peak Phosphatic Shale Member of the Permian Phosphoria Formation. It comprises part of the overburden that is removed to reach the phosphate ore at mines in SE Idaho and therefore comprises a part of the waste-rock dumps. In addition, the Rex Chert is used to surface roads in the mining district. It has been proposed by land-use managers that the chert be used to cap and isolate waste-rock dumps to prevent the release of selenium (Se) and other potentially toxic elements to the environment. Critical to this issue is that previous spot analyses of the Rex Chert indicated that Se might occur in high concentrations in some chert beds. Further, seleniferous cherts occur in other areas; for example, the Lower Permian carbonaceous cherts of Hubei Province in China average about 0.16% Se (Yao and Gao, 2002). Consequently, we sampled several outcrop sections to determine the composition of the Rex Chert.

We did not sample all beds in each outcrop, but each bed analyzed was sampled through its entire thickness. One outcrop section sampled also includes the overlying Cherty Shale Member of the Phosphoria Formation and another section includes the upper

part of the Meade Peak Phosphatic Shale Member and the transition zone between the Meade Peak and Rex Chert Members.

PREVIOUS STUDIES

The Rex Chert Member was named after Rex Peak in the Crawford Mountains in Utah (Richards and Mansfield, 1912; see discussion by Hein et al., Chapter 2). Mansfield (1927) provided the first broad discussion of the Rex Chert and characterized it as having regular bedding, fine-grained texture, uniform composition, paucity of fossils (except abundant sponge spicules in one bed), and a great thickness and areal extent. He concluded that the Rex Chert was deposited as a gelatinous mass of inorganic silica in shallow water and that the bedding resulted from minor climatic oscillations that disrupted the deposition of this vast layer of silica gel. The silica was ultimately derived from river input. Keller (1941) provided excellent petrographic descriptions of the Rex Chert and showed that the chert contains various amounts of carbonate (calcite, dolomite), carbonate fluorapatite (CFA), detrital minerals (quartz, mica), carbonaceous matter, and in places sponge spicules. The proportion of each phase depended on the paleogeographic setting in which the siliceous sediment accumulated. He concluded that the bedded chert formed from precipitation of silica gel from seawater and that chert nodules in carbonates formed by diagenetic replacement. Sheldon (1957) suggested that cherts composed of sponge spicules are the result of winnowing out of fine-grained clastic material on the seafloor. He found that pyrite and glauconite occur in some chert beds and also concluded that much of the silica in the cherts migrated during diagenesis. He found that sponge spicules commonly dissolved and the silica was re-deposited in the chert; cherts where spicules were not present showed textural evidence for diagenetic recrystallization. McKelvey et al. (1959) correctly surmised that the source of silica for the Rex Chert was biosilica that dissolved during diagenesis and only the larger, more robust spicules remained as fossils. They further recognized that chert, along with black shale and phosphorite, are upwelling indicators and that nutrient-rich upwelled waters were important in supplying silica for the silica-secreting organisms. Cressman and Swanson (1964) showed that the Rex Chert likely formed by a relatively early diagenetic process involving the transformation of biosilica (opal) to quartz, possibly through an intermediate cristobalite or tridymite stage. This mineral transformation in which biogenic opal (opal-A) transforms to opal-CT, which then transforms to quartz with increasing temperature and time is now well established (e.g. Murata et al., 1977).

The Rex Chert is Wordian in age (Guadalupian; Wardlaw and Collinson, 1984; see Hein, Chapter 1) and was part of a global episode of expanded accumulation of siliceous sediments that lasted for about 10 Ma (Murchey and Jones, 1992; Murchey, Chapter 5). The phosphorite and chert of the Phosphoria Formation were deposited in a zone of upwelling (McKelvey et al., 1959), which varied in intensity both temporally and spatially. We suggest that the phosphorites were deposited under a more intense upwelling regime, which produced suboxic bottom-water conditions (Perkins and Piper, Chapter 4), whereas

the sponges that were the source of silica for the chert thrived under conditions of moderate upwelling that allowed the bottom waters to remain oxic.

METHODS

Field sampling

This region of southeast Idaho has supported extensive phosphate mining over the past several decades and currently has four active mines. Ten sections of Rex Chert located in the vicinity of Dry Valley, northeast of Soda Springs in SE Idaho (Fig. 14-1 and Table 14-1), were described in the field during June 2001. Three of the sections (1, 5, 7) were measured and sampled in detail (Fig. 14-2) for chemical, mineralogical, and petrographic analyses. The samples within the measured sections represented the entire thickness of individual beds, where possible. Where beds were too thick to collect in their entirety, portions of beds were collected. This approach provided an opportunity to determine the changes in composition of a single rock type through the history of deposition of the stratigraphic sections. The beds sampled were intended to be representative of each section. In addition, unusual rock types were sampled, for example a large dolomitic body in the Cherty Shale Member. About 0.1–1 kg of rock was collected from each sampled bed.

TABLE 14-1

GPS coordinates and elevations; both accurate within <15 m (49 ft)

Section number	Latitude (N)	Longitude (W)	Elevation (m)
1	42° 42.16'	111° 29.07'	2122
2	42° 41.78'	111° 24.61'	1967
3	42° 42.82'	111° 21.93'	1974
4	42° 42.17'	111° 22.04'	1961
5 ¹	42° 39.38'	111° 19.76'	2042
5 ²	42° 39.39'	111° 19.42'	2042
7	42° 43.91'	111° 17.37'	2248
8	42° 42.15' ³	111° 17.07' ³	2560 ³
9	42° 44.85'	111° 17.79'	2100
10	42° 37.55'	111° 21.13'	2314
11	42° 36.89'	111° 20.25'	2134

¹ Southwest end.

² Northwest end.

³ Taken from topographic map.

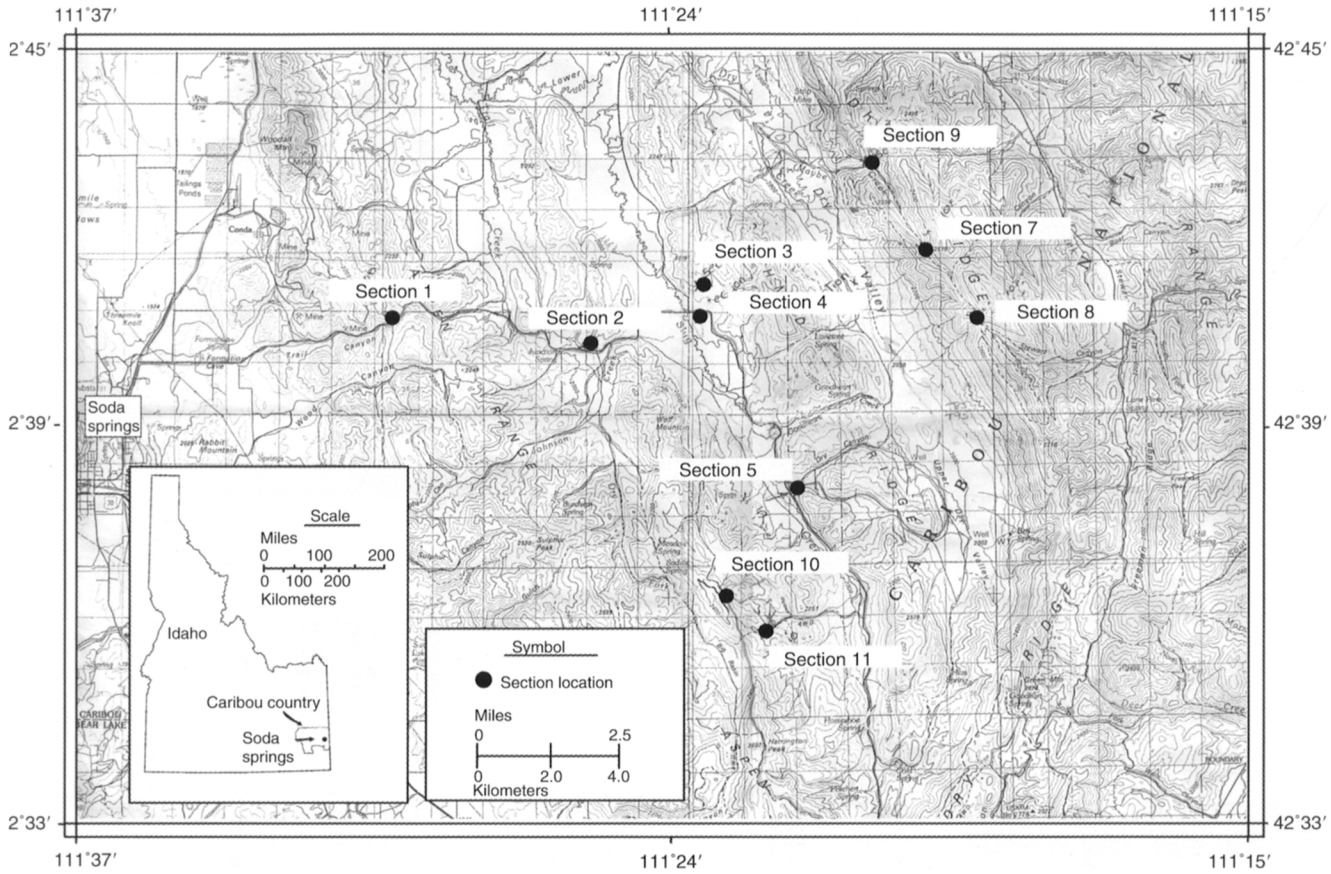


Fig. 14-1. Index map of Southeast Idaho and location of sections of Rex Chert (1-5, 7-11); sections 1, 5, and 7 were measured and sampled.

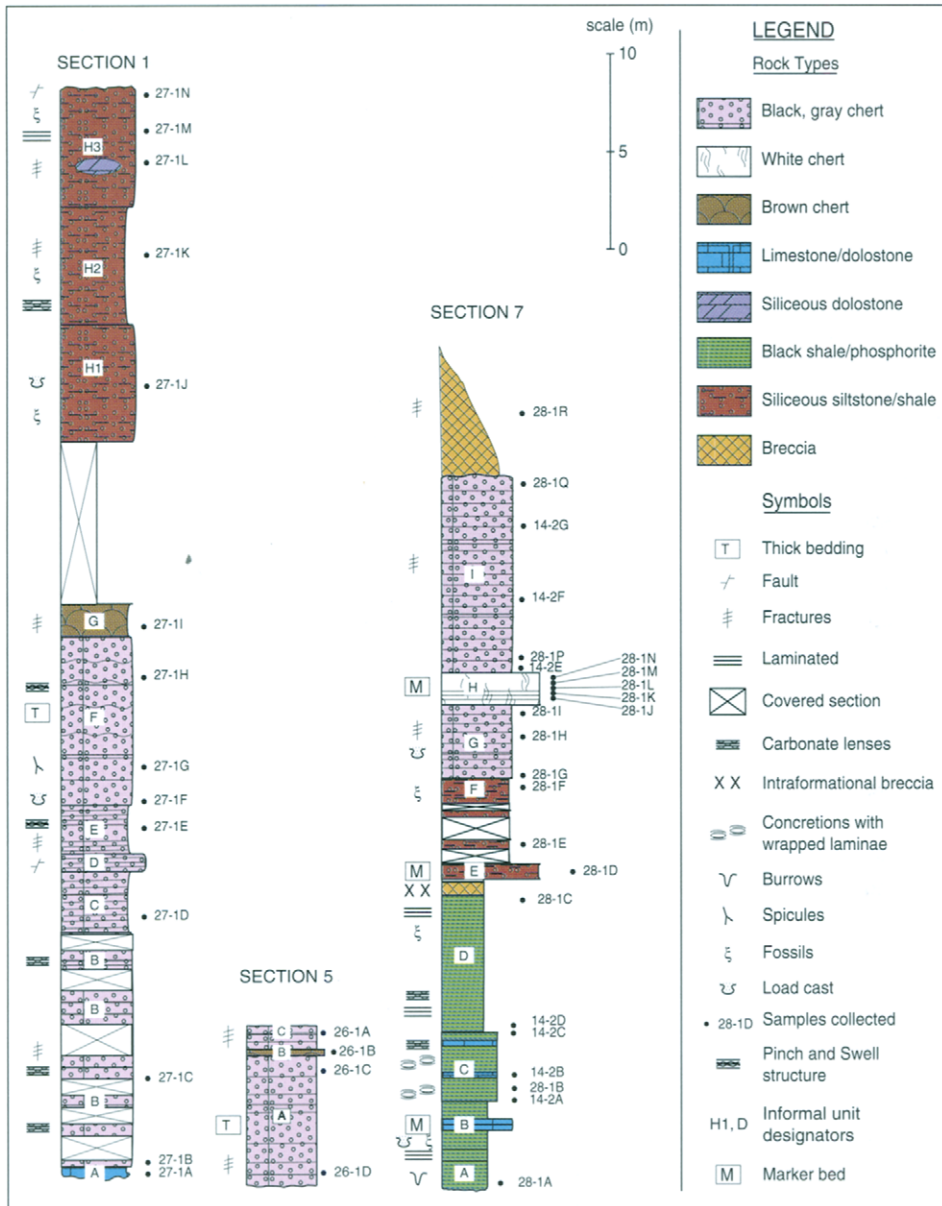


Fig. 14-2. Measured and sampled sections of Rex Chert: units H1–H3 in section 1 belong to the overlying Cherty Shale Member; units A–D in section 7 belong to the underlying Meade Peak Member; location of samples indicated to right of columns.

Rock sample preparation

A representative slab was cut through the entire thickness of each sample, crushed in a mechanical-jaw crusher, and then powdered in a roller mill. A riffle splitter was used to ensure homogenous subsamples. An aliquot of the powdered material was analyzed by X-ray diffraction for mineral content. A second aliquot of 15–50 g was sent to a contract laboratory for chemical analyses. The remaining powders for all samples are archived at the USGS. A second slab of each chert-bed sample was cut into one or more thin sections for petrographic analysis.

Geochemical analyses

Samples were analyzed for 40 major, minor, and trace elements (ICP-40) using acid digestion in conjunction with inductively coupled plasma-atomic emission spectrometry (ICP-AES; Jackson et al., 1987). Also, Sr and Ba concentrations were determined by both techniques and the two data sets are closely comparable ($R^2 = 0.999$ for Sr and 0.997 for Ba). The ICP-40 technique measures concentrations of the following elements above the indicated detection limits: Au, 8 ppm; Bi 50 ppm; Sn, 50 ppm; Ta, 40 ppm; and U, 100 ppm; however, no sample had a concentration above these quantification limits and those elements are not reported.

Another split of each sample was fused with lithium metaborate and then analyzed by ICP-AES after acid dissolution of the fusion mixture. This technique, ICP-16, provides analysis of all major elements, including Si, and a few minor and trace elements. Accuracy of Si determinations is probably about 2–4% based on the total-oxide sums. Titanium and Cr were determined using both ICP techniques, but only data from the ICP-16 technique are reported because the fusion technique more completely digests resistant minerals that might contain those elements.

Selenium, As, Sb, and Tl concentrations were determined using hydride generation followed by atomic absorption (AA) spectrometry. The hydride analytical technique is considered to be more sensitive than the acid digestion ICP-AES technique and is the source of the data reported here. Mercury was determined by cold-vapor AA spectrometry.

Total S and total C were measured using combustion in oxygen followed by infrared measurement of the evolved gas. For other forms of carbon, carbonate carbon was measured as evolved CO₂ after acidification and organic carbon was calculated as the difference between total and carbonate carbon. The compilations by Arbogast (1996) and Baedeker (1987) include additional discussions about the analytical methods used here.

Statistical analyses

The concentration of each element is reported as received from the analysts. However, qualified data (detection limit values) were modified for use in statistical analyses. An

element was not used in statistical analyses if more than 30% of the data points for that particular element were qualified. If there were fewer than 30% qualified values for an element, then the qualified values were multiplied by 0.5 and data for that element were used in the statistical analyses. Statistical analyses were performed on the combined data from all three sections (except for the Meade Peak in section 7 and the two carbonate beds in section 1) and separately for the individual data sets from sections 1 and 7. The Pearson product-moment correlation coefficient was used to calculate correlation coefficient matrices. A 99% confidence level was used to calculate the zero-point of correlation. For Q-mode factor analysis, each variable percentage was scaled to the percent of the maximum value before the values were row-normalized and cosine-theta coefficients calculated. Factors were derived from orthogonal rotations of principal-component eigenvectors using the Varimax method (Klovan and Imbrie, 1971). All communalities are ≥ 0.90 .

Mineralogical analysis

Mineral compositions were determined by X-ray diffraction using a Philips diffractometer with a graphite monochromator and Cu α radiation. Samples were run from $4-70^\circ 2\theta$ at 40 kV, 45 mA, and 10 counts per second. Semiquantitative mineral contents were determined and are grouped in Table 14-II under the classifications of major (>25%), moderate (5-25%), and minor (<5%).

RESULTS

Lithostratigraphy

The Phosphoria Formation in the Soda Springs area consists of three members which, in ascending order, are the Meade Peak Phosphatic Shale, the Rex Chert, and the Cherty Shale (McKelvey et al., 1959; Montgomery and Cheney, 1967; Brittenham, 1976; Oberlindacher, 1990). The Meade Peak unconformably overlies the Grandeur Tongue of the Permian Park City Formation, and the Cherty Shale Member is overlain by the Triassic Dinwoody Formation. The measured sections of this chapter focus on the Rex Chert; the Cherty Shale Member was measured in one section.

The contacts between the Meade Peak and the Rex Chert and between the Rex Chert and the Cherty Shale are gradational. The transitional rocks generally contain carbonates or carbonate-rich beds. Section 1 was measured through a road cut that exposed the Rex Chert and an adjacent quarry wall that exposed the Cherty Shale Member. Section 5 was measured in a small quarry where the Rex Chert was being mined for surfacing roads. The underlying Meade Peak was not exposed and the overlying Cherty Shale was not present. Section 7 was measured along the exposed face of the now-abandoned South Maybe Canyon Mine and includes the upper Meade Peak rocks and transition rocks that comprise the lowermost part of the Rex Chert. Measurements record true thickness of strata.

TABLE 14-II

X-ray diffraction mineralogy of Rex Chert and associated samples

	Type and interval	Major mineral	Moderate	Minor/trace
<i>Section 1: 1J-1N = Cherty Shale Member</i>				
601-27-1N	Cherty-calcareous shale bed	Quartz	Feldspar	Dolomite, gypsum, smectite(?)
601-27-1M	Laminated siliceous shale	Quartz	Feldspar	Illite, smectite, CFA
601-27-1L2	Siliceous dolostone	Quartz	Dolomite	Calcite, feldspar, smectite(?)
601-27-1L1	Argillaceous chert bed	Quartz	Feldspar	Goethite
601-27-1K2	Argillaceous chert bed	Quartz		Dolomite, feldspar, smectite, gypsum(?)
601-27-1K	Shaly interbed	Quartz		Feldspar, smectite, illite, CFA
601-27-1J	Cherty shale bed	Quartz		Feldspar, illite, CFA, calcite, dolomite
601-27-1I	Phosphatic-ferruginous chert bed	Quartz	CFA	Clay minerals
601-27-1H	Chert bed	Quartz		Illite, CFA, smectite(?)
601-27-1G	Base of massive thick chert bed	Quartz		CFA, heulandite(?)
601-27-1F	Chert bed	Quartz		Smectite(?)
601-27-1E	Chert bed	Quartz		CFA, smectite(?), chlorite or kaolinite(?)
601-27-1D	Chert bed	Quartz		Clay mineral
601-27-1C	Chert bed	Quartz		Dolomite, calcite, smectite(?)
601-27-1B	Chert bed	Quartz		Dolomite, calcite, smectite(?)
601-27-1A	Siliceous limestone bed	Calcite	Quartz	Dolomite, smectite(?)
<i>Section 5</i>				
601-26-1A	Chert bed	Quartz		
601-26-1B	Leached zone in chert	Quartz		Kaolinite or chlorite, goethite, bixbyite
601-26-1C	Chert bed	Quartz		Illite, chlorite or kaolinite
601-26-1D	Chert bed	Quartz		Illite, chlorite or kaolinite

Continued

TABLE 14-II

	Type and interval	Major mineral	Moderate	Minor/trace
<i>Section 7: 1A-1C = Meade Peak Member</i>				
601-28-1R1	Breccia	Quartz		Dolomite
601-28-1Q	Chert bed	Quartz		CFA(?)
601-28-1P	Chert bed	Quartz		Calcite, dolomite, clay minerals
601-28-1N	1N-1K = parts of a 80 cm thick white chert bed	Quartz		
601-28-1M	Chert	Quartz		Clay minerals
601-28-1L	Chert	Quartz		Smectite(?)
601-28-1K	Chert	Quartz		Smectite(?)
601-28-1J3	Chert	Quartz		CFA(?)
601-28-1J2	Chert	Quartz		
601-28-1J1	Chert	Quartz		Smectite(?)
601-28-1I	Chert bed	Quartz		CFA(?)
601-28-1H	Chert bed	Quartz		CFA(?), smectite(?)
601-28-1G1	Chert	Quartz		CFA(?), gypsum
601-28-1G2	Chert	Quartz		CFA, clay minerals
601-28-1G3	Chert	Quartz		CFA, smectite
601-28-1F	Phosphatic cherty shale bed	Quartz	CFA	Illite, smectite(?)
601-28-1E	Siliceous siltstone	Quartz	Plagioclase	Illite
601-28-1D	Siliceous siltstone, marker bed	Quartz	Feldspar	Illite, smectite(?), jarosite(?)
601-28-1C	Phosphatic-calcareous shale	Quartz	CFA, calcite, feldspar	Illite, natrojarosite
601-28-1B	Carbonate nodule in black shale	Calcite	Dolomite, CFA	Quartz
601-28-1A	Black phosphatic shale	Quartz	Feldspar, CFA	Calcite, dolomite, illite, pyrite

Feldspar, K-feldspar plus plagioclase; clay minerals, undifferentiated mixed-layer clay minerals.

In section 1, the Meade Peak Member is covered and the lowermost beds exposed include limestone alternating with black chert (Fig. 14-2, unit A). Most of the lower part of the Rex Chert is thin-bedded black and gray chert, which gives way up section to thick-bedded massive gray chert (units B–F). Load casts occur at the base of the thick chert. The uppermost massive chert beds are composed of composite beds displaying pinch-and-swell structures (unit F). Above the uppermost massive thick-chert bed are several thin, iron-rich, weathered chert beds (unit G). Thin sections reveal that most of the Rex Chert in this section is spiculite.

The transition to the overlying Cherty Shale Member is covered in the measured section, but in the outcrop on the opposite (south) side of the road, that position may be occupied by a chert-pebble conglomerate that is not seen on the north side of the road. The lower third of the Cherty Shale Member consists of thin-bedded (≤ 6 cm) siliceous shale, with some beds displaying load casts (unit H1). Beds generally thicken up section. The middle third of the section consists of thin-bedded (6–15 cm) argillaceous chert with thinner (< 1 –3 mm) interbedded siliceous shale (unit H2). The upper third of the section consists of moderately thick-bedded (10–30 cm) argillaceous chert with siliceous-shale partings commonly being shear surfaces (unit H3). Near the top of unit H3, a 0.5 m thick body of pale-brown siliceous dolostone appears to be the hinge of a fold. The remainder of the bed(?) is not exposed laterally from that body. This was probably originally a dolostone bed or laterally extensive lens. A bed (40 cm thick) of laminated and sheared black siliceous shale occurs near the top of the section, which is capped by a nodular siliceous-shale bed. The upper part of the section is highly sheared and is likely bounded by a fault. It is also likely that the thickness of the Rex Chert Member and Cherty Shale Member has been altered by folding and faulting. Bedding (S_0) in much of the Rex Chert has been obscured by development of generally low-relief stylolites (S_1) oriented subparallel to bedding. Locally, bedding has been transposed (S_2) so that it parallels axial planes of isoclinal folds that may have formed during compaction, or possibly during emplacement of the Paris thrust plate (see Evans, Chapter 6). S_2 remained an active structural element as shown by quartz veins that formed perpendicular to S_2 and are offset along S_2 .

Section 5 was measured at its northwest end in a quarry where the thickness of the Rex Chert is a minimum because the lower part of the section is covered and the upper part has been removed by quarrying. The Rex Chert consists of dark-gray, medium- to thick-bedded chert that is divided into two sections by an intervening friable brown layer of ferruginous chert (unit B) with an earthy texture. This 30–40 cm thick brown zone may be alteration along a fault or leaching of a chert bed. The chert in this section is spiculite, as determined from thin sections. The chert shows bedding-parallel pressure-solution cleavage as indicated by truncated microfossils and accumulations of relatively insoluble components such as sericite and hematite.

In section 7, the upper part of the Meade Peak Member (units A–D, Fig. 14-2) and transitional rock in the Rex Chert (units E–F) are well exposed. Alternating beds of black shale, phosphorite, and carbonate characterize the Meade Peak exposure. Carbonates (calcite and dolomite) occur as continuous beds, horizons of disconnected concretions, and as isolated concretions in some shale beds. Generally, the carbonates thicken up section from nodules to thin beds to thicker beds, except near the base of the exposed section where a distinctive

0.6 m thick carbonate “marker bed” occurs. These marker beds crop out over a distance of about 3 miles (4.8 km) in the North, Middle, and South Maybe Canyon mines in the Dry Ridge Mountains. Shale and phosphorite laminae wrap around the carbonate concretions indicating an early diagenetic origin (pre-compaction). The Meade Peak is overlain by a 0.8 m thick marker bed of siliceous siltstone (Fig. 14-2, unit E). That bed is overlain by a section that is partly covered, but consists predominantly of thin-bedded siliceous siltstone (unit F). That transition zone of siliceous siltstone is overlain by thin- to medium-bedded (5–30 cm) black chert with brown upper and lower margins on each bed (unit G). Load casts occur at the base of some beds. A few thin siliceous-siltstone beds also occur in unit G. Those cherts are overlain by 1 m of thin-bedded white chert that is overlain by a 1 m thick white chert marker bed (unit H). The white cherts are overlain by 10 m of thin- to medium-bedded (to 30 cm) black and gray chert (unit I) that is very similar to cherts in unit G. The section is capped by an 8 m thick, discontinuous chert megabreccia with a calcite-bearing quartz cement. This breccia body may be a slump deposit or fault-zone deposit.

Petrography

The dominant characteristic of the chert beds is the presence of sponge spicules, which vary from relatively well preserved to faint ghosts. Most beds can be classified as spiculites. These spiculites are laminated and commonly show a preferred orientation of elongate grains parallel to bedding. One sample (601-28-1H) shows preferred orientation in some laminae but not in others, indicating that the alignment of grains was caused by bottom currents rather than by compaction or tectonics. A sparse to common occurrence of rhombs characterize most spiculite beds, which are likely quartz-replaced dolomite. Glauconite, mica, and feldspar are present in some beds. Various combinations of bivalves, fish debris, radiolarians(?), and calcareous algae(?), are seen in some beds. Spiculite beds in section 7 show sedimentary structures that include cross bedding and cut-and-fill scouring.

The upper part of section 7 does not consist of spiculite beds, but rather replaced carbonates. These chert beds are generally white to grayish, centimeters to a meter thick, and in thin section consist of abundant rhombs partly to completely replaced by quartz. Some replaced rhombs show relict carbonate twinning. Laminae are compacted around some large rhombs, which indicates that they formed prior to compaction. The textures suggest that carbonate and silica fossils were deposited on the seafloor, dolomite rhombs formed in unconsolidated sediment during early diagenesis, compaction took place with increasing burial, and finally carbonate grains were replaced and cement was precipitated during silica diagenesis.

The Cherty Shale Member from section 1 consists of siliceous-siltstone beds and one siliceous-dolostone bed. Beds are laminated, contain ghosts of spicules, and some beds contain various combinations of sparse rhombs, bivalves, fish debris, feldspar, fibrous clay minerals, and calcite. Carbonate minerals are more common than they are in the underlying chert. Grains are well sorted. Uncommon sedimentary structures include burrows and reverse grading.

The siliceous siltstone from the Meade Peak–Rex Chert transition zone (lower Rex Chert) in section 7 is somewhat different from the siliceous siltstone in section 1. The section 7

siltstone is more compacted and shows a preferred fabric created by aggregate extinction of clay minerals, or by parallel orientation of thin wavy iron-rich or organic matter-rich lenses. Grains are moderately well sorted and range from angular to subrounded, but are predominantly subangular. Similar to section 1, siltstone beds are laminated, contain ghosts of spicules, and some beds contain various combinations of bivalves, fish debris, feldspar, and fibrous clay minerals, as well as mica and chlorite; however, no rhombs or calcite were seen.

Mineralogy

The mineral content of the Rex Chert and Cherty Shale Member is dominated by quartz (Table 14-II). Several beds also have major amounts of carbonate minerals. For example, the lowermost bed in section 1 (601-27-1A) contains major amounts of calcite as well as quartz; a siliceous dolostone (601-27-1L2) in section 1 contains major amounts of dolomite as well as quartz. Feldspar (combined K-feldspar and plagioclase), dolomite, and carbonate fluorapatite (CFA) occur in moderate amounts in a few beds (Table 14-II). Clay minerals occur in minor amounts. In the upper part of the Meade Peak Member in section 7, calcite is a major phase in some samples and CFA is moderately abundant in all samples analyzed.

Chemical composition

The mean concentrations of elements in the Rex Chert and the Cherty Shale Members are overwhelmingly dominated by silica, which averages 94.6% for the three sections studied and ranges from 92.2% for section 1 to 96.9% for section 5 (Table 14-III). The sums of the major oxides are reasonably close to 100%, but are a little high for most of the stratigraphically highest 13 samples from section 7, as much as 103% (Table 14-III). These high values provide a measure of the analytical accuracy of silica determinations for these very silica-rich rocks. Samples with low sums of the major oxides result from the exclusion in those totals of organic C and S compounds, which are significant components of the Meade Peak rocks in section 7.

Organic C contents are generally very low in the chert, but are as much as 1.8% in samples from the Cherty Shale Member in section 1 and as much as 3.4% in samples from the transitional rocks (lower Rex Chert) in section 7 (Table 14-III). Similarly, phosphate (P_2O_5) is generally low in the chert, but can be high (as much as 3.1%) in individual beds; these beds do not consistently occur at any particular stratigraphic level in the sections.

Selenium concentrations for samples of the Rex Chert and Cherty Shale Members vary from the detection limit (<0.2) to 138 ppm, with a mean concentration of 7 ppm (Table 14-IV), or <1.0 ppm if two outliers are removed. The mean Se concentration for section 5 rocks (0.65 ppm) is equivalent to that of average shale, 0.6 ppm (Krauskopf, 1979), whereas that of section 1 (1.32 ppm) is 2.2 times the concentration in average shale and section 7 (12 ppm) is 20 times the average-shale concentration (Tables 14-V–14-VII). The reason for these differences is that section 7 includes the lowermost Rex Chert, which contains rocks of transitional character, and section 1 includes the Cherty Shale Member. All chert beds

TABLE 14-III

Chemical composition of rocks from three sections (1, 5, 7; Figs 14-1 and 14-2) of Rex Chert and adjacent rocks; samples are listed in stratigraphic order; major oxides, C, and S in wt.%, others in ppm

Lab no.	Sample no.	Sample description	Lithology	SiO ₂ ICP-16	Al ₂ O ₃ ICP-16	Fe ₂ O ₃ ICP-16	TiO ₂ ICP-16	CaO ICP-16	K ₂ O ICP-16	MgO ICP-16	Na ₂ O ICP-16	P ₂ O ₅ ICP-16	ΣCO ₂ Acid.	Total
<i>Section 1: Rex Chert 1A 1I; Cherty Shale Member 1J 1N</i>														
C-197024	601-27-1N	Brown, calcareous	Cherty-calcareous shale bed	87.5	3.27	0.77	0.217	2.28	0.61	1.09	0.63	0.48	1.69	98.6
C-197023	601-27-1M	Black	Laminated siliceous shale	78.7	8.41	2.66	0.550	0.98	1.95	0.80	0.59	0.69	0.03	95.4
C-197022	601-27-1L2	Pale brown to gray = fresh	Siliceous dolostone	48.8	1.13	0.71	0.067	16.2	0.16	9.91	0.22	0.16	23.4	100.8
C-197021	601-27-1L1	Brown, earthy, porous	Argillaceous chert bed	92.6	2.74	1.92	0.167	0.43	0.30	0.18	0.61	0.32	0.02	99.3
C-197020	601-27-1K2	Brown, calcareous	Argillaceous chert bed	92.0	2.40	0.64	0.167	1.41	0.43	0.73	0.31	0.23	1.15	99.5
C-197019	601-27-1K	Brown	Shaly interbed	90.9	3.48	0.96	0.234	0.84	0.64	0.32	0.42	0.44	0.23	98.5
C-197018	601-27-1J	Brown, calcareous	Cherty shale bed	86.2	3.82	1.16	0.234	2.01	0.78	0.95	0.49	0.44	1.58	97.7
C-197017	601-27-1I	Brown, Fe stained	Phosphatic-feruginous chert bed	83.2	2.55	4.68	0.117	3.69	0.64	0.45	0.08	3.05	0.08	98.5
C-197016	601-27-1H	Gray	Chert bed	98.2	0.79	0.76	0.017	0.50	0.13	0.07	0.04	0.37	0.02	100.9
C-197015	601-27-1G	Gray, spicular	Base of massive thick chert bed	95.6	1.19	1.43	0.033	0.97	0.22	0.12	0.03	0.85	0.02	100.5
C-197014	601-27-1F	Gray	Chert bed	99.9	0.26	0.23	<0.020	0.39	0.02	<0.02	0.01	0.28	0.01	101.1
C-197013	601-27-1E	Gray	Chert bed	96.3	0.62	0.44	<0.020	1.27	0.08	0.05	0.03	0.96	0.02	99.7
C-197012	601-27-1D	Black	Chert bed	98.2	0.60	0.33	0.017	0.21	0.10	0.05	0.04	0.09	0.03	99.7
C-197011	601-27-1C	Black, calcareous	Chert bed	97.5	0.43	0.19	0.017	1.12	0.06	0.18	0.04	0.16	0.79	100.5
C-197010	601-27-1B	Black, calcareous	Chert bed	93.5	0.59	0.17	0.033	2.31	0.07	0.93	0.05	0.28	2.15	100.1
C-197009	601-27-1A	Gray	Siliceous limestone bed	44.3	0.19	0.06	<0.020	30.9	0.04	0.48	0.04	0.05	25.1	101.1
<i>Section 5</i>														
C-197005	601-26-1A	Dark gray, fractured	Chert bed	98.6	0.55	0.31	0.017	0.22	0.07	0.05	0.04	0.14	0.02	100.0
C-197006	601-26-1B	Earthy, brown	Leached zone in chert	93.9	1.49	2.65	0.083	0.43	0.17	0.12	0.04	0.30	0.01	99.2
C-197007	601-26-1C	Dark gray, fractured	Chert bed	97.5	1.04	0.47	0.033	0.29	0.16	0.10	0.05	0.18	0.03	99.9
C-197008	601-26-1D	Dark gray, fractured	Chert bed	97.5	1.10	0.49	0.050	0.25	0.18	0.08	0.07	0.14	0.01	99.9
<i>Section 7: Meade Peak 1A 1C; Rex Chert 1D 1R</i>														
C-197045	601-28-1R1	Pale brown-gray chert clast	Breccia	99.5	0.38	0.07	<0.020	1.05	0.05	0.55	0.05	0.14	1.10	102.9
C-197044	601-28-1Q	Dark gray, fractured	Chert bed	101.0	0.38	0.06	<0.020	0.46	0.04	0.02	0.05	0.28	0.02	102.3
C-197043	601-28-1P	Gray, mottled	Chert bed	96.7	0.25	0.04	<0.020	2.92	0.01	0.70	0.04	0.09	2.78	103.5
C-197042	601-28-1N	White, upper 15 cm margin	1N-1K = parts of a 80 cm thick	102.0	0.28	0.17	<0.020	0.28	0.04	0.02	0.04	0.18	0.01	103.1
C-197041	601-28-1M	White, middle 7 cm	White chert bed	101.8	0.32	0.04	<0.020	0.18	0.01	0.02	0.03	0.09	0.01	102.5
C-197040	601-28-1L	White, 7-15 cm above base	Chert	101.4	0.23	0.13	<0.020	0.27	<0.01	0.02	0.03	0.16	0.01	102.2
C-197039	601-28-1K	White, lower margin (8 cm)	Chert	101.6	0.36	0.10	<0.020	0.35	0.02	0.02	0.03	0.23	0.02	102.7
C-197036	601-28-1J1	Pale brown, upper bed margin	Chert	100.3	0.28	0.14	<0.020	0.28	0.02	0.02	0.04	0.18	<0.01	101.3
C-197037	601-28-1J2	White-gray, main bed, dense	Chert	101.6	0.32	0.04	<0.020	0.20	0.02	<0.02	0.03	0.11	<0.01	102.3
C-197038	601-28-1J3	White-gray, lower bed margin	Chert	101.2	0.42	0.09	<0.020	0.34	0.02	0.02	0.03	0.21	0.01	102.3
C-197035	601-28-1I	Black-brown	Chert bed	96.7	0.77	0.21	0.033	0.50	0.10	0.03	0.08	0.32	0.02	98.8
C-197034	601-28-1H	Pale brown, silty	Chert bed	99.5	0.43	0.17	0.017	0.34	0.05	0.03	0.07	0.23	0.02	100.8
C-197031	601-28-1G1	Pale brown, upper bed margin	Chert	96.0	1.38	0.37	0.050	1.01	0.22	0.08	0.12	0.69	0.05	100.0
C-197032	601-28-1G2	Brown, main bed	Chert	90.7	0.93	0.26	0.050	0.67	0.14	0.05	0.11	0.39	0.02	93.3
C-197033	601-28-1G3	Pale brown, lower bed margin	Chert	95.4	1.64	0.57	0.083	1.48	0.27	0.12	0.12	1.01	0.07	100.8
C-197030	601-28-1F	Gray-brown, fossiliferous	Phosphatic cherty shale bed	89.0	3.48	1.24	0.183	2.46	0.69	0.30	0.15	1.72	0.11	99.3
C-197029	601-28-1E	Black, thin-bedded	Siliceous siltstone	74.9	10.7	2.09	0.784	0.17	2.58	0.65	1.20	0.09	>0.01	93.1
C-197028	601-28-1D	Gray-brown, mid. thick bed	Siliceous siltstone, marker bed	78.5	11.1	0.96	0.817	0.34	2.57	0.61	1.32	0.05	<0.01	96.3
C-197027	601-28-1C	Black	Phosphatic-calcareous shale	48.3	8.35	2.75	0.484	17.1	1.88	0.70	0.66	5.50	8.18	93.9
C-197026	601-28-1B	Black nodule	Carbonate nodule in black shale	1.07	0.15	0.06	<0.020	48.7	0.01	3.30	0.11	2.75	39.3	95.4
C-197025	601-28-1A	Black, carbonaceous	Black phosphatic shale	46.0	7.29	2.37	0.484	11.1	1.94	1.44	1.21	4.42	5.49	81.7

Sample no.	C _T Comb.	C _i Acid.	C _{org} Difference	S _T Comb.	Ag ICP-40	As Hydride	Ba ICP-40	Ba ICP-16	Be ICP-40	Cd ICP-40	Ce ICP-40	Co ICP-40	Cr ICP-16	Cu ICP-40	Eu ICP-40	Ga ICP-40	Hg CVAA	Ho ICP-40	La ICP-40
601-27-1N	1.32	0.46	0.86	0.2	<2	3.1	593	611	<1	<2	19	<2	172	32	<2	<4	0.05	<4	20
601-27-1M	1.81	0.01	1.80	0.05	<2	12.6	243	243	2	<2	36	3	759	56	<2	14	0.15	<4	31
601-27-1L2	6.36	6.39	-0.03	<0.05	<2	1.1	28	27	<1	<2	6	<2	95	29	<2	<4	0.02	<4	8
601-27-1L1	0.11	0.01	0.10	<0.05	<2	3.8	57	60	<1	<2	12	<2	137	20	<2	<4	0.04	<4	10
601-27-1K2	0.77	0.31	0.46	0.12	<2	2.5	480	439	<1	<2	13	<2	139	23	<2	<4	0.04	<4	10
601-27-1K	0.76	0.06	0.70	<0.05	<2	3.8	138	125	<1	<2	19	2	224	49	<2	4	0.03	<4	16
601-27-1J	1.57	0.43	1.14	0.07	<2	3.1	123	124	<1	<2	20	3	300	31	<2	5	0.03	<4	17
601-27-1I	0.31	0.02	0.29	<0.05	<2	13.2	78	81	2	<2	87	<2	1100	36	8	8	0.14	7	176
601-27-1H	0.13	0.01	0.12	<0.05	<2	6.1	86	80	<1	<2	9	<2	106	13	<2	<4	0.02	<4	18
601-27-1G	0.13	0.01	0.12	<0.05	<2	5.1	39	48	<1	<2	10	<2	170	23	<2	<4	0.04	<4	14
601-27-1F	0.01	<0.003	0.007	<0.05	<2	0.9	18	16	<1	<2	5	<2	23	11	<2	<4	<0.02	<4	12
601-27-1E	0.27	0.01	0.26	<0.05	<2	2.5	30	30	<1	<2	5	<2	67	27	<2	<4	0.05	<4	19
601-27-1D	0.39	0.01	0.38	<0.05	<2	1.3	50	49	<1	<2	5	<2	86	152	<2	<4	0.04	<4	3
601-27-1C	0.38	0.22	0.16	<0.05	<2	0.7	26	27	<1	<2	5	<2	19	33	<2	<4	0.02	<4	3
601-27-1B	0.91	0.59	0.32	<0.05	<2	1.0	25	24	<1	<2	5	<2	39	30	<2	<4	0.02	<4	7
601-27-1A	7.06	6.85	0.21	<0.05	<2	<0.6	8	>10	<1	<2	5	<2	12	24	<2	<4	0.02	<4	3
601-26-1A	0.09	0.01	0.08	<0.05	<2	1.6	273	261	<1	<2	5	<2	51	24	<2	<4	0.02	<4	5
601-26-1B	0.11	<0.003	0.107	<0.05	<2	14.5	85	84	<1	<2	8	<2	72	60	<2	<4	0.10	<4	10
601-26-1C	0.13	0.01	0.12	<0.05	<2	2.7	127	115	<1	<2	5	<2	81	32	<2	<4	0.03	<4	4
601-26-1D	0.19	<0.003	0.187	0.05	<2	2.4	423	415	<1	<2	6	<2	74	13	<2	<4	0.03	<4	6
601-28-1R1	0.38	0.30	0.08	<0.05	<2	4.3	27	32	<1	<2	5	<2	15	9	<2	<4	0.02	<4	3
601-28-1Q	0.11	0.01	0.10	<0.05	<2	5.4	25	26	<1	<2	5	<2	12	6	<2	<4	0.02	<4	3
601-28-1P	0.81	0.76	0.05	<0.05	<2	<0.6	17	23	<1	<2	5	<2	>10	10	<2	<4	0.02	<4	3
601-28-1N	0.02	<0.003	0.017	<0.05	<2	0.9	21	28	<1	<2	5	<2	20	148	<2	<4	0.02	<4	5
601-28-1M	0.01	<0.003	0.007	<0.05	<2	<0.6	24	26	<1	<2	5	<2	>10	8	<2	<4	0.02	<4	3
601-28-1L	0.03	<0.003	0.027	<0.05	<2	2.8	21	22	<1	<2	5	<2	10	93	<2	<4	0.02	<4	4
601-28-1K	0.02	0.01	0.01	<0.05	<2	0.9	25	33	<1	2	5	<2	15	40	<2	<4	0.02	<4	6
601-28-1J1	0.03	<0.003	0.027	<0.05	<2	2.3	35	37	<1	2	5	<2	12	122	<2	<4	0.02	<4	4
601-28-1J2	0.02	<0.003	0.017	<0.05	<2	0.8	39	44	<1	<2	5	<2	11	7	<2	<4	0.02	<4	3
601-28-1J3	0.03	<0.003	0.027	<0.05	<2	1.2	37	40	<1	<2	5	<2	13	12	<2	<4	0.02	<4	6
601-28-1I	0.15	0.01	0.14	<0.05	<2	2.1	43	43	<1	<2	5	<2	48	10	<2	<4	0.03	<4	9
601-28-1H	0.12	0.01	0.11	<0.05	<2	0.6	29	33	<1	<2	8	<2	13	33	<2	<4	0.03	<4	6
601-28-1G1	0.18	0.01	0.17	<0.05	3	6.6	51	50	<1	4	7	<2	148	154	<2	<4	0.04	<4	18
601-28-1G2	0.35	0.01	0.34	0.05	<2	4.1	62	56	<1	4	5	<2	102	34	<2	<4	0.06	<4	12
601-28-1G3	0.21	0.02	0.19	<0.05	3	11.0	62	59	<1	11	10	<2	234	296	<2	<4	0.05	<4	29
601-28-1F	0.18	0.03	0.15	<0.05	3	16.8	108	108	1	22	19	<2	601	52	<2	6	0.05	<4	48
601-28-1E	3.35	<0.003	3.347	0.42	<2	14.2	342	336	1	47	42	<2	452	38	<2	6	0.16	<4	29
601-28-1D	0.76	<0.003	0.757	0.18	6	1.9	365	351	1	7	46	<2	135	52	<2	13	0.10	<4	26
601-28-1C	4.62	2.23	2.39	0.29	<2	23.2	367	346	1	5	62	8	589	67	4	12	0.17	<4	140
601-28-1B	13.8	10.73	3.07	0.27	<2	3.3	14	11	<1	15	<5	<2	153	41	<2	<4	0.03	<4	11
601-28-1A	13.3	1.50	11.8	2.97	15	32.2	223	212	2	37	52	4	1800	183	2	15	0.59	<4	84

Continued

TABLE 14-III *Continued*

Sample no.	Li ICP-40	Mn ICP-40	Mo ICP-40	Nb ICP-40	Nd ICP-40	Ni ICP-40	Pb ICP-40	Sb Hydride	Sc ICP-40	Se Hydride	Sr ICP-40	Sr ICP-16	Th ICP-40	Ti Hydride	V ICP-40	Y ICP-40	Yb ICP-40	Zn ICP-40	Zr ICP-16
601-27-1N	14	81	<2	<4	25	37	9	0.7	3	2.8	85	92	<6	0.1	32	36	2	110	95
601-27-1M	27	76	<2	<4	37	97	7	0.6	9	0.9	66	70	7	0.5	86	49	3	154	164
601-27-1L2	16	298	<2	6	10	14	4	<0.6	<2	0.4	124	126	<6	<0.1	14	13	<1	28	31
601-27-1L1	29	333	<2	<4	13	45	<4	<0.6	3	0.9	23	26	<6	0.3	27	20	2	112	70
601-27-1K2	17	68	3	<4	14	29	5	<0.6	2	1.8	64	65	<6	0.1	20	16	<1	49	72
601-27-1K	13	60	<2	<4	22	40	7	0.6	4	1.9	52	56	<6	0.1	31	31	2	98	101
601-27-1J	12	91	<2	<4	22	44	6	0.9	4	2.4	63	65	<6	0.1	37	32	2	99	91
601-27-1I	43	31	<2	4	197	21	13	2.2	3	2.2	215	231	<6	0.1	188	321	13	52	42
601-27-1H	8	13	<2	<4	21	10	<4	<0.6	<2	0.9	27	30	<6	<0.1	24	30	1	43	<10
601-27-1G	8	16	<2	<4	30	13	<4	<0.6	<2	1.2	34	40	<6	0.3	38	54	3	135	18
601-27-1F	5	16	<2	<4	12	4	<4	<0.6	<2	0.4	16	17	<6	<0.1	4	16	<1	30	<10
601-27-1E	6	38	<2	<4	23	21	<4	<0.6	<2	1.9	44	47	<6	<0.1	21	46	2	78	15
601-27-1D	9	42	2	<4	<9	20	9	0.6	<2	0.8	14	14	<6	<0.1	19	8	<1	133	<10
601-27-1C	4	37	<2	<4	<9	8	<4	<0.6	<2	<0.2	23	23	<6	<0.1	5	6	<1	57	13
601-27-1B	4	50	<2	<4	<9	11	<4	<0.6	<2	0.3	34	36	<6	<0.1	14	13	<1	81	16
601-27-1A	4	148	<2	<4	<9	4	4	<0.6	<2	<0.2	188	183	<6	<0.1	5	3	<1	32	<10
601-26-1A	6	29	<2	<4	<9	8	<4	0.9	<2	0.6	22	23	<6	<0.1	11	10	<1	29	<10
601-26-1B	10	1710	<2	<4	15	98	5	1.0	<2	0.6	24	28	<6	0.3	35	20	1	244	45
601-26-1C	13	36	<2	<4	11	11	<4	0.7	<2	0.5	24	27	<6	<0.1	15	12	<1	45	27
601-26-1D	10	22	<2	<4	9	13	<4	0.7	<2	0.9	51	54	<6	<0.1	18	13	<1	50	23
601-28-1R1	5	106	<2	<4	<9	6	<4	0.8	<2	<0.2	19	21	<6	<0.1	5	5	<1	38	12
601-28-1Q	4	21	<2	<4	<9	5	<4	<0.6	<2	0.2	17	17	<6	<0.1	3	5	<1	24	<10
601-28-1P	4	160	<2	<4	<9	23	<4	<0.6	<2	<0.2	15	15	<6	<0.1	<2	4	<1	73	<10
601-28-1N	5	92	<2	<4	<9	8	<4	<0.6	<2	<0.2	11	15	<6	<0.1	3	7	<1	121	13
601-28-1M	<2	57	<2	<4	<9	4	<4	<0.6	<2	<0.2	8	<10	<6	<0.1	<2	3	<1	28	<10
601-28-1L	3	191	<2	<4	<9	10	<4	<0.6	<2	<0.2	10	11	<6	<0.1	3	6	<1	109	12
601-28-1K	13	221	<2	<4	<9	11	<4	<0.6	<2	<0.2	12	13	<6	<0.1	5	8	<1	94	21
601-28-1J1	4	299	<2	<4	<9	20	<4	1.0	<2	<0.2	14	15	<6	<0.1	3	6	<1	153	<10
601-28-1J2	4	250	<2	<4	<9	15	<4	<0.6	<2	<0.2	12	15	<6	<0.1	<2	4	<1	62	<10
601-28-1J3	7	227	<2	<4	<9	21	<4	<0.6	<2	<0.2	15	17	<6	<0.1	4	8	<1	79	<10
601-28-1I	6	48	<2	<4	<9	13	<4	0.7	<2	2.5	29	32	<6	<0.1	13	15	<1	91	14
601-28-1H	6	107	<2	<4	<9	13	58	11.4	<2	0.7	16	17	<6	<0.1	5	9	<1	90	<10
601-28-1G1	12	55	<2	<4	13	31	6	1.0	<2	1.3	43	46	<6	0.7	47	29	1	253	19
601-28-1G2	8	51	2	<4	<9	29	<4	<0.6	<2	2.9	36	35	<6	0.4	27	19	<1	123	13
601-28-1G3	16	58	<2	<4	21	45	<4	0.8	3	1.3	58	60	<6	0.8	63	44	2	437	24
601-28-1F	18	34	<2	<4	37	86	5	1.5	4	3.8	95	97	<6	0.9	130	76	4	569	52
601-28-1E	21	32	12	<4	18	33	14	1.8	8	138	80	83	12	1.3	122	10	2	96	394
601-28-1D	18	24	<2	5	20	25	13	0.9	7	101	78	82	9	1.0	63	9	2	115	397
601-28-1C	21	496	14	5	93	251	13	1.8	9	17.2	275	282	<6	1.1	110	206	10	658	233
601-28-1B	<2	69	18	4	16	27	6	0.9	<2	6.1	696	699	<6	<0.1	280	21	<1	201	23
601-28-1A	31	146	65	11	59	361	14	6.2	9	99.5	437	436	<6	1.1	196	144	8	1460	243

TABLE 14-IV

Statistics of chemical data for 36 Rex Chert and Cherty Shale samples collected from measured sections 1, 5, and 7; for comparison mean values for 9 Rasmussen Ridge mine and 13 Enoch Valley mine composite channel Rex Chert samples

Element	<i>N</i>	Mean	Median	SD	Minimum	Maximum	Rasmussen mean ²	Enoch mean ²
SiO ₂ (wt %)	36	94.6	96.7	7.07	74.9	102	75.6	81.8
Al ₂ O ₃	36	1.92	0.78	2.73	0.23	11.1	7.19	6.47
Fe ₂ O ₃	36	0.75	0.35	0.98	0.04	4.68	2.45	2.68
TiO ₂	36	0.11	0.033	0.20	< 0.01	0.817	0.40	0.36
CaO	36	0.91	0.48	0.88	0.17	3.69	2.65	0.99
K ₂ O	36	0.37	0.115	0.65	0.005	2.58	1.71	1.42
MgO	36	0.27	0.09	0.33	0.01	1.09	1.37	0.55
Na ₂ O	36	0.20	0.05	0.32	0.01	1.32	0.52	0.34
P ₂ O ₅	36	0.43	0.255	0.56	0.05	3.05	1.42	1.03
ΣCO ₂	36	0.34	0.02	0.69	0.005	2.78	1.65	0.05
Total	36	99.9	100	2.46	93.1	103.5	95.0	95.7
C _t	36	0.45	0.18	0.67	0.01	3.35	3.70	1.31
C _c	36	0.09	0.01	0.19	< 0.0015	0.76	0.45	0.01
C _{org}	36	0.35	0.13	0.63	0.007	3.35	3.24	1.30
S _t	36	0.05	0.025	0.08	< 0.025	0.42	1.34	0.16
As (ppm)	36	4.37	2.6	4.59	0.3	16.8	11.2	11.0
Ba	36	117	50.5	147.5	17	593	192	166
Ba	36	116	49.5	144	16	611	191	171
Ce	36	12	5	17.4	< 2.5	87	33.4	26.4
Cr	36	152	73	234	5	1100	525	297
Cu	36	50	32	58.8	6	296	51.9	45.2
Hg	36	0.04	0.03	0.04	< 0.01	0.16	0.26	0.16
La	36	17	9.5	29.2	3	176	41.4	26.1
Li	36	11	8	8.62	1	43	21.7	20.7
Mn	36	133	56	283	13	1710	142	98.8
Nd	36	18	10	32.2	< 4.5	197	41.6	33.1
Ni	36	26	20	24.0	4	98	148	94.7
Sb	36	0.94	0.6	1.85	< 0.3	11.4	0.81	0.49
Se	36	7.60	0.85	27.9	< 0.1	138	62.9	18.3
Sr	36	40.2	25.5	38.5	8	215	107	88.8
V	36	31.2	18.5	41.4	< 1	188	122	90.0
Y	36	27.8	13	53.1	3	321	62.5	47.4
Zn	36	115	92.5	110	24	569	375	282
Zr	36	51	15.5	92.1	< 5	397	116	102

R.I. Grauch and J.R. Herring, unpublished data.

TABLE 14-V

Statistics of chemical data for 14 Rex Chert and Cherty Shale samples collected from measured section 1

Element	N	Mean	Median	SD	Minimum	Maximum
SiO ₂ (wt %)	14	92.2	93.05	6.28	78.7	99.9
Al ₂ O ₃	14	2.23	1.795	2.18	0.26	8.41
Fe ₂ O ₃	14	1.17	0.765	1.24	0.17	4.68
TiO ₂	14	0.130	0.075	0.150	< 0.01	0.55
CaO	14	1.315	1.05	0.964	0.21	3.69
K ₂ O	14	0.431	0.26	0.509	0.02	1.95
MgO	14	0.424	0.25	0.393	0.01	1.09
Na ₂ O	14	0.241	0.065	0.253	0.01	0.63
P ₂ O ₅	14	0.617	0.405	0.744	0.09	3.05
ΣCO ₂	14	0.559	0.055	0.765	0.01	2.15
Total	14	99.3	99.6	1.50	95.4	101
C _i	14	0.634	0.385	0.580	0.01	1.81
C _c	14	0.154	0.015	0.208	< 0.0015	0.59
C _{org}	14	0.480	0.305	0.498	0.007	1.8
S _i	14	0.049	0.025	0.051	< 0.025	0.2
As (ppm)	14	4.26	3.1	3.98	0.7	13.2
Ba	14	142	67.5	179	18	593
Ba	14	140	70	177	16	611
Ce	14	16.96	11	22.3	< 2.5	87
Cr	14	239	138	310	19	1100
Cu	14	38.3	30.5	34.9	11	152
Hg	14	0.047	0.04	0.044	< 0.01	0.15
La	14	25.4	15	44.0	3	176
Li	14	14.2	10.5	11.4	4	43
Mn	14	68	46	80.2	13	333
Nd	14	30.7	21.5	48.9	< 4.5	197
Ni	14	28.6	21	24.0	4	97
Sb	14	0.571	0.3	0.509	< 0.3	2.2
Se	14	1.32	1.05	0.842	< 0.1	2.8
Sr	14	54.3	39	51.0	14	215
V	14	39	25.5	47.2	< 4	188
Y	14	48.4	30.5	79.9	6	321
Zn	14	87.9	89.5	38.4	30	154
Zr	14	51	30	48.9	< 5	164

in the upper part of section 7 have Se concentrations of <0.2–0.8 ppm. The mean concentration of 12 ppm is heavily dependent on two sample values of 101 and 138 ppm. Without those two samples, the mean Se concentration in section 7 rocks would be 0.8 ppm, close to the average-shale content.

TABLE 14-VI

Statistics of chemical data for four Rex Chert samples collected from measured section 5

Element	N	Mean	Median	SD	Minimum	Maximum
SiO ₂ (wt %)	4	96.9	97.5	2.05	93.9	98.6
Al ₂ O ₃	4	1.05	1.07	0.386	0.55	1.49
Fe ₂ O ₃	4	0.98	0.48	1.12	0.31	2.65
TiO ₂	4	0.046	0.0415	0.028	0.017	0.083
CaO	4	0.298	0.27	0.093	0.22	0.43
K ₂ O	4	0.145	0.165	0.051	0.07	0.18
MgO	4	0.088	0.09	0.030	0.05	0.12
Na ₂ O	4	0.05	0.045	0.014	0.04	0.07
P ₂ O ₅	4	0.19	0.16	0.076	0.14	0.3
ΣCO ₂	4	0.018	0.015	0.010	0.01	0.03
Total	4	99.8	99.9	0.370	99.2	100
C _t	4	0.13	0.12	0.043	0.09	0.19
C _c	4	0.006	0.006	0.005	<0.0015	0.01
C _{org}	4	0.124	0.114	0.045	0.08	0.187
S _t	4	0.031	0.025	0.0125	0.025	0.05
As (ppm)	4	5.3	2.55	6.15	1.6	14.5
Ba	4	227	200	154	85	423
Ba	4	219	188	152	84	415
Ce	4	5.375	5.5	2.29	2.5	8
Cr	4	69.5	73	12.9	51	81
Cu	4	32.2	28	20.1	13	60
Hg	4	0.045	0.03	0.037	0.02	0.1
La	4	6.25	5.5	2.63	4	10
Li	4	9.75	10	2.87	6	13
Mn	4	449	32.5	841	22	1710
Nd	4	9.88	10	4.37	4.5	15
Ni	4	32.5	12	43.7	8	98
Sb	4	0.825	0.8	0.15	0.7	1
Se	4	0.65	0.6	0.173	0.5	0.9
Sr	4	30.2	24	13.9	22	51
V	4	19.8	16.5	10.6	11	35
Y	4	13.8	12.5	4.35	10	20
Zn	4	92	47.5	102	29	244
Zr	4	25	25	16.4	<5	45

Other elements of environmental interest include As, Cr, V, Zn, Hg, and Cd. Arsenic concentrations vary by a factor of 56, from 0.3 to 16.8 ppm, with a mean of 4.2 ppm, which is slightly less than the concentration in average shale of 6.6 ppm (Govett, 1983). Chromium concentrations vary by a factor of 220, from 5 to 1100 ppm, with a mean of

TABLE 14-VII

Statistics of chemical data for 18 Rex Chert samples collected from measured section 7

Element	N	Mean	Median	SD	Minimum	Maximum
SiO ₂ (wt. %)	18	95.9	99.5	7.99	74.9	102
Al ₂ O ₃	18	1.87	0.4	3.38	0.23	11.1
Fe ₂ O ₃	18	0.375	0.155	0.542	< 0.04	2.09
TiO ₂	18	0.118	0.01	0.252	0.01	0.817
CaO	18	0.739	0.345	0.796	0.17	2.92
K ₂ O	18	0.381	0.045	0.815	0.005	2.58
MgO	18	0.182	0.03	0.256	0.01	0.7
Na ₂ O	18	0.197	0.05	0.389	0.03	1.32
P ₂ O ₅	18	0.343	0.195	0.418	0.05	1.72
ΣCO ₂	18	0.237	0.02	0.684	< 0.005	2.78
Total	18	100	102	3.19	93.1	104
C _t	18	0.376	0.135	0.780	0.01	3.35
C _c	18	0.066	0.01	0.187	< 0.0015	0.76
C _{org}	18	0.309	0.09	0.779	0.007	3.35
S _t	18	0.057	0.025	0.098	< 0.025	0.42
As (ppm)	18	< 4.25	2.2	4.93	< 0.3	16.8
Ba	18	74.1	36	104	17	365
Ba	18	74.8	38.5	99.8	22	351
Ce	18	9.42	2.5	14.1	< 2.5	47
Cr	18	103	15	169	5	601
Cu	18	62.4	36	75.9	6	296
Hg	18	0.034	0.01	0.040	< 0.01	0.16
La	18	12.1	6	12.8	3	48
Li	18	8.61	6	6.10	1	21
Mn	18	113	75	88.7	21	299
Nd	18	9.31	4.5	9.10	< 4.5	37
Ni	18	22.1	17.5	19.4	4	86
Sb	18	1.25	0.5	2.57	< 0.3	11.4
Se	18	< 14	0.15	38.9	< 0.1	138
Sr	18	31.6	16.5	27.7	8	95
V	18	27.7	5	41.4	< 1	130
Y	18	15	8	18.4	3	76
Zn	18	142	95	143	24	569
Zr	18	56	12.5	124	< 5	397

143 ppm, which is higher than the 100 ppm concentration in average shale. Vanadium concentrations vary by a factor of 188, from 1 to 188 ppm, with a mean of 30 ppm, which is much lower than the 130 ppm concentration in average shale. Zinc concentrations vary by a factor of 24, from 24 to 569 ppm, with a mean of 110 ppm, which is somewhat greater than

the concentration in average shale of 80 ppm. Mercury concentrations vary by a factor of 16, from < 0.01 to 0.16 ppm, with a mean of 0.04 ppm, which is an order-of-magnitude less than the concentration in average shale of 0.4 ppm. Cadmium concentrations are uniformly below the limit of quantification (< 2 ppm) except for rocks from the lowermost part of section 7; we are unable to ascertain whether the average may be higher than the 0.3 ppm of average shale.

Stratigraphic changes in chemical composition

Stratigraphic changes (equivalent to temporal changes in the depositional basin) in the chemical composition of rocks are notable either as uniform changes through the sections or as distinct differences in the mean composition of rocks that comprise the upper and lower halves of the sections. In this regard, the concentrations of most elements increase up section at the expense of silica in section 1, whereas they decrease up section in sections 5 and 7. The up-section increases in section 1 are partly due to inclusion of the Cherty Shale Member samples. However, there are still up-section increases in roughly half the elements even if the Cherty Shale samples are excluded. Silica has the opposite trend of the other elements. For section 1 (including the Cherty Shale Member), the following elements increase up section: Al, Fe, Ti, K, Na, As, Ba, Ce, Cr, Hg, La, Li, Ni, Sc, Sr, V, and Zr; in contrast, silica decreases up section and Ca, Mg, C, and Mn decrease to near mid-section then increase farther up section. For section 5, the following elements decrease up section: Al, Fe, Ti, K, Na, C, Ce, Ni, Sr, V, Y, and Zn; whereas Si increases up section. For section 7, the following elements decrease up section: Al, Fe, Ti, K, Na, organic C, Ba, Ce, Cr, La, Li, Ni, Se, Sr, Tl, V, Y, Zn, and Zr; whereas Si and Mn increase up section.

Phase associations of elements

The phase associations of elements were determined by comparing results from element correlations (Tables 14-VIII–14-X), rotated factor loadings from Q-mode factor analyses (Figure 14-3), and mineralogy as determined by XRD (Table 14-II). Three data sets were analyzed including data from sections 1, 5, and 7 combined, section 1 data, and section 7 data (excluding Meade Peak and Rex Chert carbonate beds).

We consider four to five Q-mode factors that account for 95% or more of the variance in each of the three data sets. The factors are interpreted to represent the following rock and mineral components. Factor 1 is a chert-silica component consisting solely of Si, except for the combined data set where Ba shows a minor but statistically significant factor loading. Factor 2 is a phosphorite-carbonate fluorapatite component composed of P, Ca, As, Y, V, Cr, Sr, and La (\pm Fe, Zn, Cu, Ni, Li, Se, Nd, and Hg depending on the data set). Factor 3 is a shale component composed of Al, Na, Zr, K, Ba, Li, and organic C (\pm Ti, Mg, Se, Ni, Fe, Sr, V, Mn, and Zn depending on the data set). Factor 4 is a

TABLE 14-VIII

Correlation coefficient matrix for 36 samples from sections 1, 5, and 7 combined (listed in TABLE 14-III); the point of zero correlation for $n = 36$ at the 99% confidence level is |0.421|

Element	SiO ₂	Al ₂ O ₃	Fe ₂ O ₃	TiO ₂	CaO	K ₂ O	MgO	Na ₂ O	P ₂ O ₅	CO ₂	C _c	C _i	C _{org}	S _T	As	Ba	Ce	Cr	Cu	Hg	La	Li	Mn
Al ₂ O ₃	-0.905																						
Fe ₂ O ₃	-0.686	0.504																					
TiO ₂	-0.882	0.995	0.451																				
CaO	-0.369	0.048	0.398	0.007																			
K ₂ O	-0.897	0.995	0.494	0.992	0.047																		
MgO	-0.682	0.545	0.314	0.542	0.617	0.534																	
Na ₂ O	-0.824	0.937	0.357	0.951	-0.012	0.915	0.566																
P ₂ O ₅	-0.347	0.083	0.68	0.013	0.679	0.091	0.098	-0.086															
CO ₂	-0.11	-0.061	-0.146	-0.044	0.643	-0.068	0.739	0.038	-0.117														
C _T	-0.784	0.758	0.348	0.764	0.211	0.768	0.734	0.735	-0.051	0.334													
C _c	-0.108	-0.064	-0.149	-0.047	0.641	-0.071	0.736	0.035	-0.119	1	0.332												
C _{org}	-0.798	0.821	0.413	0.823	0.033	0.835	0.558	0.768	-0.018	0.056	0.96	0.054											
S _T	-0.673	0.746	0.232	0.775	-0.029	0.757	0.497	0.805	-0.14	0.089	0.822	0.086	0.844										
As	-0.574	0.462	0.731	0.407	0.307	0.456	0.178	0.251	0.604	-0.229	0.343	-0.232	0.433	0.263									
Ba	-0.546	0.557	0.204	0.564	0.077	0.539	0.543	0.607	-0.073	0.158	0.509	0.153	0.493	0.653	0.126								
Ce	-0.806	0.691	0.838	0.659	0.444	0.708	0.448	0.577	0.65	-0.074	0.488	-0.078	0.54	0.462	0.566	0.355							
Cr	-0.72	0.529	0.851	0.464	0.558	0.539	0.389	0.324	0.812	-0.091	0.416	-0.094	0.468	0.222	0.742	0.216	0.866						
Cu	0.036	0.003	-0.03	-0.008	-0.018	0.001	-0.165	-0.039	0.131	-0.198	-0.079	-0.201	-0.024	-0.077	0.233	-0.13	-0.025	0.066					
Hg	-0.861	0.779	0.823	0.748	0.202	0.787	0.373	0.618	0.444	-0.205	0.616	-0.207	0.714	0.565	0.732	0.397	0.816	0.764	0.078				
La	-0.501	0.27	0.789	0.219	0.615	0.292	0.212	0.125	0.909	-0.1	0.122	-0.103	0.16	0.082	0.558	0.072	0.861	0.864	0.044	0.599			
Li	-0.715	0.577	0.854	0.526	0.408	0.555	0.361	0.491	0.659	-0.134	0.35	-0.137	0.412	0.288	0.609	0.338	0.846	0.851	0.08	0.75	0.772		
Mn	0.068	-0.083	0.277	-0.077	-0.141	-0.118	-0.111	-0.098	-0.107	-0.07	-0.14	-0.072	-0.127	-0.107	0.288	-0.11	-0.104	-0.127	0.034	0.158	-0.102	-0.025	
Nd	-0.451	0.21	0.807	0.157	0.613	0.23	0.212	0.071	0.896	-0.076	0.083	-0.079	0.112	0.018	0.499	0.066	0.836	0.84	-0.014	0.56	0.984	0.755	-0.074
Ni	-0.552	0.468	0.56	0.423	0.244	0.42	0.325	0.325	0.295	-0.023	0.326	-0.026	0.353	0.116	0.729	0.217	0.304	0.514	0.198	0.586	0.2	0.477	0.501
Sb	-0.028	0.024	0.063	0.025	-0.021	0.037	-0.061	0.016	0.086	-0.109	0.009	-0.108	0.041	0.04	0.032	-0.039	0.145	0.078	-0.008	0.118	0.114	0.056	4.56E-04
Se	-0.642	0.805	0.225	0.837	-0.168	0.827	0.284	0.814	-0.136	-0.115	0.663	-0.117	0.736	0.868	0.26	0.397	0.498	0.19	-0.024	0.576	0.107	0.263	-0.095
Sr	-0.718	0.493	0.77	0.446	0.665	0.501	0.465	0.377	0.822	0.04	0.362	0.036	0.373	0.329	0.59	0.4	0.903	0.881	0.022	0.689	0.916	0.812	-0.167
V	-0.762	0.604	0.825	0.549	0.512	0.614	0.335	0.421	0.794	-0.149	0.428	-0.152	0.498	0.375	0.816	0.243	0.882	0.936	0.14	0.811	0.854	0.828	-0.075
Y	-0.384	0.116	0.766	0.057	0.642	0.134	0.154	-0.027	0.938	-0.082	0.007	-0.085	0.033	-0.068	0.498	-0.002	0.77	0.821	0.02	0.499	0.978	0.717	-0.085
Zn	-0.194	0.159	0.165	0.116	0.247	0.129	-0.021	0.036	0.391	-0.14	-0.038	-0.142	0.002	-0.056	0.624	-0.064	0.061	0.311	0.601	0.209	0.153	0.218	0.183
Zr	-0.825	0.963	0.385	0.98	-0.053	0.963	0.492	0.955	-0.058	-0.047	0.742	-0.05	0.8	0.832	0.333	0.552	0.621	0.356	-0.028	0.694	0.173	0.455	-0.059
	Nd	Ni	Sb	Se	Sr	V	Y	Zn															
Ni	0.168																						
Sb	0.091	-0.004																					
Se	0.022	0.054	0.064																				
Sr	0.887	0.323	0.08	0.266																			
V	0.793	0.496	0.098	0.405	0.897																		
Y	0.99	0.164	0.095	-0.069	0.866	0.775																	
Zn	0.058	0.652	0.047	-0.01	0.214	0.436	0.12																
Zr	0.109	0.303	0.022	0.915	0.395	0.488	0.005	0.05															

TABLE 14-IX

Correlation coefficient matrix for 14 samples from section I (listed in TABLE 14-III): the point of zero correlation for n = 14 at the 99% confidence level is |0.651|

Element	SiO ₂	Al ₂ O ₃	Fe ₂ O ₃	TiO ₂	CaO	K ₂ O	MgO	Na ₂ O	P ₂ O ₅	CO ₂	C _T	C _C	C _{org}	S _T	As	Ba	Ce	Cr	Cu	Hg	La	Li	Mn	
Al ₂ O ₃	-0.884																							
Fe ₂ O ₃	-0.717	0.514																						
TiO ₂	-0.858	0.993	0.436																					
CaO	-0.573	0.136	0.523	0.105																				
K ₂ O	-0.895	0.984	0.549	0.968	0.19																			
MgO	-0.697	0.548	0.132	0.58	0.608	0.535																		
Na ₂ O	-0.666	0.784	0.234	0.814	0.055	0.672	0.592																	
P ₂ O ₅	-0.476	0.134	0.851	0.05	0.704	0.212	0.012	-0.148																
CO ₂	-0.181	-0.004	-0.322	0.053	0.502	-0.027	0.806	0.233	-0.257															
C _T	-0.754	0.774	0.101	0.8	0.322	0.776	0.863	0.669	-0.114	0.551														
C _C	-0.175	-0.008	-0.326	0.048	0.498	-0.032	0.803	0.229	-0.261	1	0.547													
C _{org}	-0.805	0.906	0.254	0.912	0.167	0.918	0.67	0.683	-0.023	0.224	0.937	0.22												
S _T	-0.344	0.293	-0.1	0.338	0.313	0.251	0.684	0.562	-0.135	0.564	0.53	0.558	0.385											
As	-0.738	0.644	0.907	0.566	0.383	0.707	0.151	0.22	0.732	-0.377	0.236	-0.379	0.434	-0.081										
Ba	-0.432	0.436	0.002	0.482	0.247	0.395	0.654	0.605	-0.103	0.429	0.547	0.422	0.461	0.947	0.076									
Ce	-0.737	0.458	0.94	0.393	0.695	0.516	0.26	0.18	0.894	-0.151	0.186	-0.157	0.282	0.04	0.85	0.128								
Cr	-0.812	0.61	0.944	0.541	0.589	0.681	0.273	0.221	0.827	-0.216	0.307	-0.222	0.451	-0.026	0.927	0.089	0.961							
Cu	0.007	0.055	-0.051	0.052	-0.215	0.09	-0.107	-0.059	-0.117	-0.164	0.122	-0.166	0.212	-0.105	-0.036	-0.07	-0.026	0.058						
Hg	-0.802	0.7	0.855	0.638	0.415	0.763	0.243	0.295	0.699	-0.309	0.357	-0.313	0.547	0.056	0.912	0.198	0.817	0.919	0.163					
La	-0.512	0.167	0.869	0.094	0.717	0.244	0.074	-0.097	0.967	-0.204	-0.069	-0.209	0.008	-0.091	0.741	-0.043	0.946	0.866	-0.061	0.7				
Li	-0.722	0.56	0.928	0.511	0.446	0.55	0.204	0.429	0.702	-0.252	0.14	-0.258	0.271	0.059	0.795	0.188	0.87	0.854	-0.001	0.809	0.766			
Mn	-0.188	0.274	0.176	0.291	-0.163	0.121	0.086	0.648	-0.167	-0.01	0.031	-0.008	0.039	0.066	-0.023	0.067	-0.026	-0.038	-0.1	0.022	-0.137	0.415		
Nd	-0.517	0.178	0.883	0.101	0.708	0.254	0.063	-0.091	0.976	-0.226	-0.074	-0.231	0.011	-0.086	0.756	-0.037	0.949	0.871	-0.066	0.709	0.997	0.768	-0.142	
Ni	-0.797	0.968	0.411	0.967	-0.008	0.93	0.471	0.807	0.009	-0.05	0.739	-0.052	0.883	0.245	0.536	0.382	0.312	0.486	0.149	0.641	0.027	0.502	0.402	
Sb	-0.604	0.259	0.812	0.196	0.743	0.326	0.231	0.059	0.868	-0.051	0.141	-0.058	0.188	0.036	0.656	0.042	0.932	0.854	0.136	0.659	0.931	0.731	-0.111	
Se	-0.513	0.329	0.325	0.31	0.527	0.302	0.449	0.462	0.407	0.209	0.377	0.201	0.356	0.611	0.249	0.58	0.451	0.355	-0.087	0.311	0.369	0.355	0.025	
Sr	-0.677	0.318	0.823	0.264	0.843	0.378	0.355	0.12	0.904	0.035	0.188	0.028	0.207	0.206	0.706	0.251	0.95	0.862	-0.091	0.715	0.939	0.766	-0.118	
V	-0.698	0.421	0.955	0.343	0.663	0.493	0.181	0.082	0.927	-0.229	0.129	-0.234	0.249	-0.062	0.883	0.025	0.982	0.969	0.03	0.858	0.952	0.85	-0.064	
Y	-0.483	0.132	0.867	0.054	0.714	0.209	0.039	-0.131	0.984	-0.225	-0.108	-0.229	-0.029	-0.113	0.731	-0.073	0.93	0.848	-0.065	0.686	0.994	0.744	-0.15	
Zn	-0.393	0.546	0.148	0.526	-0.176	0.51	0.214	0.484	-0.136	-0.07	0.455	-0.067	0.559	0.091	0.207	0.108	-0.02	0.143	0.502	0.337	-0.213	0.135	0.298	
Zr	-0.843	0.959	0.384	0.976	0.145	0.908	0.627	0.89	0.023	0.14	0.801	0.134	0.878	0.442	0.469	0.569	0.363	0.47	-0.004	0.547	0.061	0.491	0.355	
		Nd	Ni	Sb	Se	Sr	V	Y	Zn															
Ni		0.034																						
Sb		0.928	0.123																					
Se		0.391	0.262	0.502																				
Sr		0.94	0.165	0.929	0.592																			
V		0.958	0.292	0.911	0.378	0.92																		
Y		0.998	-0.006	0.919	0.382	0.929	0.947																	
Zn		-0.175	0.635	-0.065	0.106	-0.137	0.047	-0.177																
Zr		0.071	0.933	0.186	0.438	0.274	0.287	0.025	0.501															

TABLE 14-X

Correlation coefficient matrix for 18 samples from section 7 (listed in Table 14-III); the point of zero correlation for $n = 18$ at the 99% confidence level is |0.582|

Element	SiO ₂	Al ₂ O ₃	Fe ₂ O ₃	TiO ₂	CaO	K ₂ O	MgO	Na ₂ O	P ₂ O ₅	CO ₂	C _T	C _C	C _{org}	S _T	As	Ba	Ce	Cr	Cu	Hg	La	Li	Mn				
Al ₂ O ₃	-0.942																										
Fe ₂ O ₃	-0.897	0.864																									
TiO ₂	-0.93	0.998	0.841																								
CaO	-0.104	-0.084	0.098	-0.12																							
K ₂ O	-0.936	0.999	0.861	0.999	-0.103																						
MgO	-0.675	0.645	0.549	0.648	0.469	0.651																					
Na ₂ O	-0.909	0.987	0.791	0.995	-0.171	0.99	0.64																				
P ₂ O ₅	-0.144	-0.007	0.325	-0.073	0.578	-0.041	-0.075	-0.155																			
CO ₂	0.057	-0.156	-0.188	-0.145	0.714	-0.148	0.616	-0.137	-0.15																		
C _T	-0.786	0.754	0.811	0.763	-0.002	0.772	0.682	0.753	-0.169	0.126																	
C _C	0.058	-0.158	-0.19	-0.146	0.713	-0.15	0.614	-0.139	-0.151	1	0.126																
C _{org}	-0.801	0.793	0.858	0.799	-0.172	0.809	0.536	0.788	-0.132	-0.113	0.971	-0.113															
S _T	-0.841	0.872	0.85	0.883	-0.218	0.888	0.584	0.879	-0.207	-0.117	0.952	-0.118	0.982														
As	-0.573	0.451	0.786	0.401	0.379	0.436	0.305	0.325	0.738	-0.161	0.479	-0.163	0.519	0.435													
Ba	-0.939	0.997	0.842	0.997	-0.125	0.997	0.626	0.991	-0.046	-0.175	0.745	-0.177	0.788	0.872	0.413												
Ce	-0.944	0.993	0.891	0.988	-0.052	0.992	0.64	0.972	0.048	-0.16	0.759	-0.162	0.799	0.869	0.497	0.987											
Cr	-0.702	0.591	0.877	0.541	0.388	0.574	0.382	0.459	0.72	-0.159	0.52	-0.161	0.559	0.51	0.935	0.555	0.637										
Cu	0.005	-0.013	0.109	-0.034	0.114	-0.027	-0.184	-0.043	0.408	-0.214	-0.115	-0.218	-0.063	-0.095	0.314	-0.031	0.012	0.196									
Hg	-0.959	0.912	0.919	0.903	-0.057	0.912	0.548	0.888	0.097	-0.199	0.847	-0.199	0.896	0.908	0.596	0.91	0.923	0.686	0.078								
La	-0.721	0.632	0.817	0.58	0.399	0.605	0.359	0.508	0.764	-0.204	0.377	-0.206	0.427	0.415	0.86	0.6	0.672	0.945	0.331	0.676							
Li	-0.806	0.775	0.853	0.741	0.19	0.758	0.447	0.697	0.479	-0.216	0.562	-0.217	0.615	0.625	0.724	0.753	0.798	0.809	0.3	0.805	0.875						
Mn	0.531	-0.443	-0.469	-0.417	-0.171	-0.43	-0.286	-0.405	-0.334	0.104	-0.312	0.103	-0.337	-0.321	-0.482	-0.414	-0.452	-0.476	-0.061	-0.526	-0.521	-0.42					
Nd	-0.641	0.587	0.757	0.534	0.46	0.559	0.377	0.457	0.785	-0.144	0.293	-0.147	0.329	0.329	0.835	0.549	0.629	0.917	0.324	0.569	0.978	0.815	-0.469				
Ni	-0.503	0.344	0.618	0.286	0.611	0.314	0.254	0.201	0.875	-0.033	0.186	-0.035	0.195	0.152	0.805	0.315	0.394	0.883	0.299	0.424	0.907	0.689	-0.284				
Sb	-0.019	0.013	0.059	0.014	-0.091	0.017	-0.06	0.023	0.011	-0.103	0.031	-0.099	0.055	0.032	-0.042	0.007	0.1	0.015	-0.063	0.101	0.019	0.024	-0.078				
Se	-0.891	0.961	0.831	0.972	-0.213	0.971	0.634	0.974	-0.21	-0.127	0.866	-0.129	0.898	0.962	0.363	0.963	0.949	0.477	-0.086	0.909	0.458	0.668	-0.357				
Sr	-0.865	0.786	0.883	0.744	0.325	0.764	0.508	0.688	0.598	-0.161	0.525	-0.163	0.565	0.574	0.816	0.763	0.811	0.907	0.221	0.808	0.963	0.9	-0.585				
V	-0.817	0.731	0.934	0.687	0.314	0.715	0.462	0.619	0.625	-0.181	0.601	-0.183	0.646	0.621	0.901	0.701	0.768	0.976	0.225	0.803	0.959	0.888	-0.528				
Y	-0.284	0.128	0.438	0.063	0.575	0.094	0.025	-0.02	0.986	-0.151	-0.062	-0.152	-0.025	-0.088	0.776	0.091	0.181	0.794	0.404	0.23	0.847	0.578	-0.382				
Zn	-0.247	0.126	0.418	0.066	0.556	0.093	0.013	-0.013	0.949	-0.145	-0.08	-0.148	-0.044	-0.096	0.737	0.089	0.181	0.746	0.593	0.205	0.824	0.58	-0.251				
Zr	-0.903	0.988	0.812	0.995	-0.174	0.993	0.646	0.997	-0.155	-0.137	0.778	-0.139	0.812	0.899	0.345	0.989	0.974	0.481	-0.056	0.887	0.511	0.706	-0.379				
	Nd	Ni	Sb	Se	Sr	V	Y	Zn																			
Ni	0.904																										
Sb	2.37E-04	-0.002																									
Se	0.394	0.16	0.024																								
Sr	0.926	0.812	0.005	0.635																							
V	0.92	0.833	0.016	0.619	0.963																						
Y	0.853	0.925	0.014	-0.079	0.703	0.719																					
Zn	0.844	0.906	0.002	-0.076	0.667	0.685	0.964																				
Zr	0.463	0.205	0.005	0.983	0.684	0.632	-0.021	-0.012																			

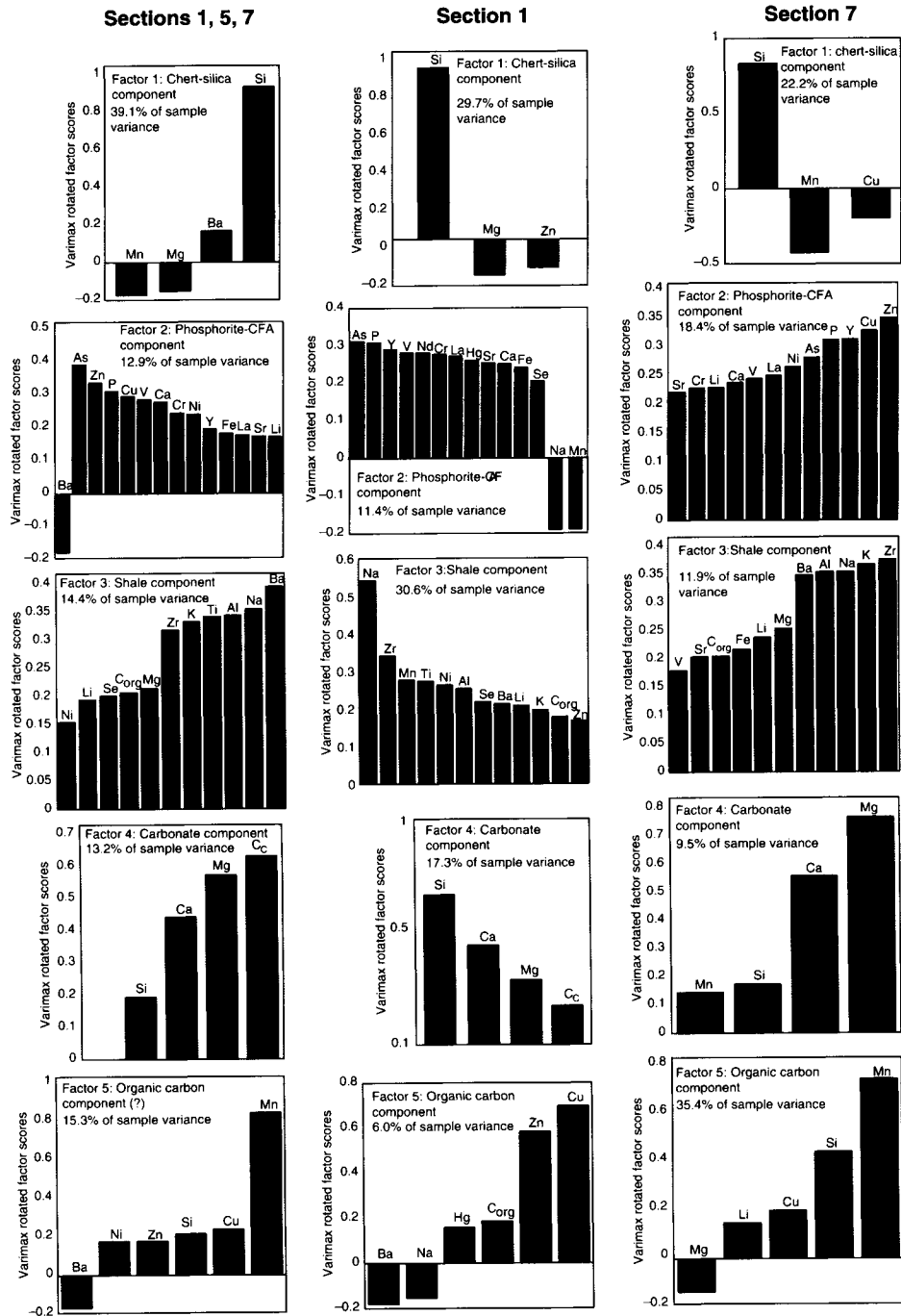


Fig. 14-3. Q-mode factors for Rex Chert and Cherty Shale samples from sections 1, 5, and 7 combined; total variance accounted for is 94.9%; section 1 only; total variance accounted for is 95.0%; section 7; total variance accounted for is 97.4%.

carbonate component (dolomite, calcite, silicified carbonates) composed of carbonate C, Mg, Ca, and Si (\pm Mn). Factor 5 is tentatively interpreted as representing organic matter (and/or sulfide–sulfate phases) hosting elements that include Cu (\pm organic C, Zn, Mn, Si, Ni, Hg, and Li depending on the data set). Copper correlates only with Zn, but Zn also correlates with Ni, As, and some elements associated with the shale component. Silica is dominantly in the chert fraction (factor 1) and does not appear in the aluminosilicate fraction (factor 3) even though it is clearly part of the feldspars and clay minerals that comprise that fraction. Likewise, organic C is dominantly in factor 3 and does not appear in factor 5 (except for section 1) even though it is possible that the elements in factor 5 are hosted by organic matter. These characteristics are an artifact of analyzing a data set that is overwhelmingly dominated by one variable, silica, and the distribution of some elements in more than one phase. Selenium shows a dominant association with the shale component, but correlations and Q-mode factors also indicate that organic matter (within the shale component) and carbonate fluorapatite may host a portion of the Se. Consideration of larger numbers of factors in Q-mode analysis indicates that native Se (a factor containing Se (\pm Ba)) may also constitute a minor component of the Se complement.

DISCUSSION AND CONCLUSIONS: ENVIRONMENTALLY SENSITIVE ELEMENTS

Analyses of outcrop samples from the Rex Chert and adjoining members of the Phosphoria Formation in southeast Idaho provide clear evidence that the chert contains low concentrations of environmentally sensitive elements, but that adjacent and transitional rocks may contain high concentrations of those elements. The chert beds have low Se concentrations, <1 ppm, whereas the Cherty Shale Member rocks have somewhat higher Se concentrations, with a mean of 1.8 ppm. Some beds in the siliceous siltstone of the lowermost Rex Chert, which comprises the zone of transition with the Meade Peak, have high Se concentrations, up to 138 ppm. These transitional beds overall comprise a small part of the Rex Chert and would be the only significant source of Se that would be released to the environment during weathering of the Rex Chert Member.

The low Se contents determined for the chert-bed samples here are not characteristic of Se concentrations found for composite channel samples taken through the Rex Chert at the Rasmussen Ridge and Enoch Valley Mines (R.I. Grauch and J.R. Herring, unpublished data, 2002). Those channel samples comprise a continuous composite record of Rex Chert composition through the entire section. Those weighted (for stratigraphic thickness) mean Se concentrations are 63 ppm for Rasmussen Ridge samples and 18 ppm for Enoch Valley samples (Table 14-IV). These differences can be explained in several ways: (a) weathering of the outcrops that we sampled; (b) the higher organic-matter contents of the composite samples, which are ninefold higher for Rasmussen Ridge samples and fourfold higher for Enoch Valley samples; (c) higher (two to threefold) CFA (P_2O_5) in the composite samples, and (d) the inclusion of shale and siliceous shale beds that may be interbedded with cherts in the analyses of composite samples. Explanation 2 is one of

the likely manifestations of explanation 1. Greater amounts of terrigenous material (explanation 4) in the composite samples is supported by their lower silica and higher Al_2O_3 , K_2O , etc., contents (Table 14-IV). In the outcrop sections studied here, shale interbedded with the chert consists only of thin partings, except in the Cherty Shale Member, and those partings would not likely contribute significantly to the mean Se concentration for each outcrop section. It is not known why there are more (or thicker) shale interbeds, or more argillaceous cherts in the composite sections than those studied in outcrops. Chert is very resistant to weathering and little Se should be leached by weathering of the outcrops. However, the most significant factor may be the much higher contents of organic matter and the moderately higher contents of CFA in the composite samples. Organic matter is commonly a host phase for metals, as indicated in our statistical analyses. Organic matter can be readily oxidized and removed during weathering, along with its associated complement of metals.

Other elements of environmental interest include As, Cr, V, Zn, Hg, and Cd. Of these elements, only mean Cr and Zn values are higher, 30 and 27% respectively, than their respective values in average shale. Cadmium could not be evaluated because most concentrations are below the limit of quantification of 2 ppm. As with Se, the concentration of these elements in our outcrop samples are lower than they are in the composite samples from the mines. The likely reason is the same as it is for Se, the higher shale component, CFA, and especially the higher organic-matter content of the mine composite samples are the hosts for these elements.

This difference in the contents of Se between the two groups of samples suggests to us that the organic fraction is indeed the dominant host of Se. This observation is consistent with that found for Permian organic C-rich, seleniferous chert in China (Yao and Gao, 2002) and for the Miocene siliceous Monterey Formation of California (Piper and Isaacs, 1995). The much lower concentrations of Se in samples of Rex Chert presented here suggest that Se and the organic matter may have been lost through weathering that extended over many years. Thus, freshly exposed outcrop samples of Rex Chert may contain higher concentrations of Se and other elements of environmental concern than samples from outcrops that have existed for extended periods of time.

These geochemical relationships are especially pronounced for the lower part of the Rex Chert where rocks are of transitional character with the Meade Peak Member and in the Cherty Shale Member rocks that overlie the Rex Chert. In the outcrop samples analyzed here, those stratigraphic intervals have higher terrigenous fraction and organic matter, Se, and trace metal concentrations than the more highly siliceous Rex Chert.

ACKNOWLEDGMENTS

We thank Richard I. Grauch, Margaret A. Keller, and Florence L. Wong for helpful reviews of this chapter. We thank R.I. Grauch and J.R. Herring for kindly providing unpublished data on composite channel samples from the Enoch Valley and Rasmussen Ridge mines. Access to those mine sites is gratefully acknowledged.

REFERENCES

- Arbogast, B.F. (ed.), 1996. Analytical methods manual for the Mineral Resource Surveys Program, US Geological Survey. US Geological Survey, Open-File Report, 96-525, 248 pp.
- Baedecker, P.A. (ed.), 1987. Methods for geochemical analysis. US Geological Survey, Bulletin, 1770, variously paginated.
- Brittenham, M.D., 1976. Permian Phosphoria carbonate banks, Idaho–Wyoming thrust belt. In: J.G. Hill (ed.), Symposium on geology of the Cordilleran hingeline. Rocky Mountain Association of Geologists – 1976 symposium, Denver, CO, pp. 173–191.
- Cressman, E.R. and Swanson, R.W., 1964. Stratigraphy and petrology of the Permian rocks of southwestern Montana: US Geological Survey, Professional Paper, 313-C, pp. 275–569.
- Govett, G.J.S., 1983. Handbook of Exploration Geochemistry, vol. 3, Rock Geochemistry in Mineral Exploration. Elsevier, Amsterdam, 461 pp.
- Jackson, L.L., Brown, F.W. and Neil, S.T., 1987. Major and minor elements requiring individual determinations, classical whole rock analysis, and rapid rock analysis. In: P.A. Baedecker (ed.), Methods for Geochemical Analysis. US Geological Survey, Bulletin, 1770, pp. G1–G23.
- Keller, W.D., 1941. Petrography and origin of the Rex Chert. *Geol. Soc. Am. Bull.*, 52: 1279–1298.
- Klován J.E. and Imbrie J., 1971. An algorithm and FORTRAN-IV program for large-scale Q-mode factor analysis and calculation of factor scores. *Math. Geol.*, 3: 61–77.
- Krauskopf, K.B., 1979. Introduction to Geochemistry. McGraw-Hill, New York, 617 pp.
- Mansfield, G.R., 1927. Geography, geology, and mineral resources of part of southeastern Idaho. US Geological Survey, Professional Paper, 152, 453 pp.
- McKelvey, V.E., Williams, J.S., Sheldon, R.P., Cressman, E.R., Cheney, T.M., and Swanson, R.W., 1959. The Phosphoria, Park City and Shedhorn Formations in western phosphate field. US Geological Survey, Professional Paper, 313-A, 47 pp.
- Montgomery, K.M. and Cheney, T.M., 1967. Geology of the Stewart Flat quadrangle, Caribou County, Idaho. US Geological Survey, Bulletin, 1217, 63 pp.
- Murata, K.J., Friedman, I., and Gleason, J.D., 1977. Oxygen isotope relations between diagenetic silica minerals in Monterey Shale, Temblor Range, California. *Am. J. Sci.*, 277: 259–272.
- Murchey, B.L. and Jones, D.L., 1992. A mid-Permian chert event: widespread deposition of biogenic siliceous sediments in coastal, island arc and oceanic basins. *Palaeogeogr. Palaeoclimatol. Palaeoecol.*, 96: 161–174.
- Oberlindacher, H.P., 1990. Geologic map and phosphate resources of the northeastern part of the Lower Valley quadrangle, Caribou County, Idaho. US Geological Survey, Miscellaneous Field Studies Map, MF-2133, scale 1:12,000.
- Piper, D.Z. and Isaacs, C.M., 1995. Geochemistry of minor elements in the Monterey Formation, California – seawater chemistry of deposition. US Geological Survey, Professional Paper, 1566, 41 pp.
- Richards, R.W. and Mansfield, G.R., 1912. The Bannock overthrust. *J. Geol.*, 20: 683–689.
- Sheldon, R.P., 1957. Physical stratigraphy of the Phosphoria Formation in northwestern Wyoming. US Geological Survey, Bulletin, 1042-E, 185 pp.
- Wardlaw, B.R. and Collinson, J.W., 1984. Conodont paleoecology of the Permian Phosphoria Formation and related rocks of Wyoming and adjacent areas. In: D.L. Clark (ed.), Conodont Biofacies and Provincialism. Geological Society of America Special Paper 196, pp. 263–281.
- Yao, L. and Gao, Z., 2002. Abnormal enrichment of selenium in Yutangba carbonaceous cherts, southeast Enshi, Hubei Province, China. Abstracts, Goldschmidt Conference 2002, *Geochim. Cosmochim. Acta*, 66: A859.